h_0 = film thickness, constant thickness region, cm.
k = fluid property coefficient, Equation (13)
L = nondimensional meniscus thickness, h/h_0
L'' = d^2L/dR^2
L''_{DL} = limiting value, dynamic region 2
L''_{SL} = limiting value, static region 3
n = fluid property coefficient, $(a_1\rho g)^\alpha$
m = fluid property coefficient, Equation (16a)
P = curvature coefficient, nondimensional, Equation (11)
P_L = large P value ($P_L > P_N$), Figure 2
P_N = Newtonian P value, constant, Figure 2
P_S = small P value ($P_S < P_N$)
P_V = very large P value ($P_V > P_L$), Equation (22)
R = nondimensional height, x/h_0
T_0 = nondimensional parameter, $h_0(a_0\rho g/u)^{1/2}$
T_1 = nondimensional parameter, $h_0[(a_1\rho g)^\alpha/u]^{1/(\alpha+1)}$
u = withdrawal speed, cm./sec.
v = local velocity, cm./sec.
w = mass flow rate, g./sec.
x = height in meniscus, cm.
y = coordinate

Greek Letters

α = rheological exponent, nondimensional, Equation (1)
μ = Newtonian viscosity, poise
ρ = density, g./cc.
σ = surface tension, dyne/cm.
τ_{yx} = shear stress, dynes/sq.cm.

LITERATURE CITED

1. Deryaguin, B. V., and S. M. Levi, "Film Coating Theory," Focal Press, New York (1964).
2. Gutfinger, Chaim, Ph.D. dissertation, Yale Univ., New Haven, Conn. (Aug. 1964).
3. ———, personal communication (Oct., 1964).
4. ———, and J. A. Tallmadge, *AIChE J.*, **11**, 403 (1965).
5. Hildebrand, R. E., and J. A. Tallmadge, *ibid.*, **14**, 660 (1968).
6. ———, *Can. J. Chem. Eng.*, **46**, 394 (1968).
7. Levich, V. G., "Physicochemical Hydrodynamics," Chapt. 12, Prentice Hall, Englewood Cliffs, N. J. (1962).
8. Tallmadge, J. A., *AIChE J.*, **12**, 1011 (1966).
9. ———, *Chem. Eng. Sci.*, **24**, 471 (1969).
10. ———, and Chaim Gutfinger, *Photo. Sci. Eng.*, **11**, 98 (1967).
11. ————————, *Ind. Eng. Chem.*, **59**, No. 11, 18 (1967). Corrections in **60**, No. 2, 74 (1968).
12. White, D. A., and J. A. Tallmadge, *Chem. Eng. Sci.*, **20**, 33 (1965).
13. ———, *AIChE J.*, **12**, 333 (1966).
14. *Ibid.*, 13, 745 (1967).

Manuscript received October 8, 1968; revision received March 6, 1969; paper accepted March 10, 1969. Paper presented at AIChE Los Angeles meeting.

Concentration Fluctuations and Chemical Conversion Associated with Mixing in Some Turbulent Flows

ROBERT S. TORREST and WILLIAM E. RANZ

University of Minnesota, Minneapolis, Minnesota

Microconductivity probes were used for the measurement of point values of mean concentrations and root-mean-square concentration fluctuations for mixing of salt solutions in turbulent shear flows. Mixing studies covered a range of flow conditions, with Reynolds numbers on the order of 10^4, and included ducted turbulent jets, dispersion in turbulent pipe flow, a plane mixing zone, and several multiple injection systems. The test sections all had characteristic dimensions of about 2 cm. The results for mixing experiments are compared with available previous work. Lack of resolution for root-mean-square concentration fluctuations in some previous work is indicated.

Reaction product concentrations for a rapid, second-order, irreversible reaction in multiple injection systems, the plane jet, and the mixing zone were also obtained. The relation between conversion in reaction experiments and fluctuation level and decay in the equivalent mixing experiments is illustrated.

The study of mass transfer in turbulent flows has, for a long time, implied the measurement of mean concentration profiles and perhaps calculation of eddy diffusion coefficients from these results. However, the concentration measured at a point in a turbulent flow in general exhibits essentially random fluctuations with various frequencies and amplitudes about the mean value. The second moment or variance of the concentration fluctuations is therefore the next bit of information needed for a more detailed look at turbulent mass transfer. In fact, the standard deviation of the concentration fluctuations, known as the *intensity*, may be of the same order of magnitude as the mean concentration.

The fluctuation intensity is particularly useful since, even with uniform mean concentration in the field, mixing

Robert S. Torrest is with Shell Development Company, Houston, Texas.

is not complete until the fluctuations are leveled by diffusion and the intensity goes to zero.

Furthermore, when one considers rapid chemical reactions in turbulent flows, it need only be noted that in the limiting case of a homogeneous field with constant mean concentration, the decay of concentration fluctuations in the mass transfer situation can be directly related to conversion in the reactor for the same flow conditions. Turbulent diffusion flames are a particularly striking example from the general class of diffusion controlled reactions. In these cases the degree of conversion depends on the rate of fluctuation decay, that is, on the extent of mixing.

This paper presents some measurements of point values of mean concentrations and root-mean-square concentration fluctuations for mixing of ionic (salt) solutions in several turbulent shear flows. Measurements were obtained with microconductivity probes, and an electrical system was developed to handle high intensity fluctuations. Mean conversion results for very rapid irreversible reactions in a few equivalent flows are also included. Comparison with previous related studies are made.

TURBULENT MIXING THEORY

The conservation equation for concentration fluctuation variance $\overline{\gamma^2}$ is

$$\frac{\partial \overline{\gamma^2}}{\partial t} + U_i \frac{\partial \overline{\gamma^2}}{\partial x_i} + 2\overline{\gamma u_i}\frac{\partial \overline{C}}{\partial x_i} + \frac{\partial}{\partial x_i}\left(\overline{u_i\gamma^2} - D\frac{\partial \overline{\gamma^2}}{\partial x_i}\right) = -2D\overline{\frac{\partial \gamma}{\partial x_i}\frac{\partial \gamma}{\partial x_i}} \quad (1)$$

This equation (for example, 33) follows from the mass conservation equation for an incompressible fluid with constant diffusivity D, where the instantaneous concentration C and velocity components U_i have been written as the sum of time mean and fluctuating parts as $C = \overline{C} + \gamma$, $U_i = \overline{U_i} + u_i$.

Equation (1) shows that fluctuation variance is produced by the interaction of the turbulent concentration flux $\overline{\gamma u_i}$ and mean gradient, undergoes turbulent and molecular diffusion, and is dissipated by molecular diffusion. Although careful detailed analyses of turbulent mass transfer would involve the term-by-term study of this equation, our knowledge of the subject is far from this goal. In fact, all that is available are a few studies of fluctuation intensity distributions in jets (for example, *1* to *4*), for dispersion in pipe flow (*5, 6*), in the wake of a line heat source (*47*), and measurements in grid generated turbulence (*7, 8*) and in stirred tanks.

It is evident that a careful study of turbulent mass transfer presupposes a detailed knowledge of the turbulent velocity fields. The turbulent energy balance (*9, 10*) has been studied in detail in many shear flows for term-by-term behavior (for example *11* to *15*), and Equation (1) has the same form.

Corrsin (*16*) carried out the first systematic treatment of isotropic scalar fields along the lines used for velocity fields. In this treatment, turbulent velocity and concentration fluctuations decay in a uniform field of mean velocity and concentration. Then, for a given point in the field, the time change of fluctuation variance must be balanced by dissipation by molecular diffusion or

$$\frac{\partial \overline{\gamma^2}}{\partial t} = -2D\overline{\frac{\partial \gamma}{\partial x_i}\frac{\partial \gamma}{\partial x_i}} = 6D\overline{\gamma^2}\left(\frac{\partial^2 m}{\partial r^2}\right)_{r=0} = -12D\frac{\overline{\gamma^2}}{\lambda_\gamma^2} \quad (2)$$

where $m(r, t) = \overline{\gamma_1\gamma_2}/\overline{\gamma^2}$ is the correlation between fluctuations at points 1 and 2, and λ_γ is the microscale (*10*) given by

$$\lambda_\gamma^2 = -2 \Big/ \left(\frac{\partial^2 m}{\partial r^2}\right)_{r=0} \quad (3)$$

Corrsin considered the application of the full correlation equation for certain special cases. The results show that scalar fluctuations die out at a slower rate than velocity fluctuations and that concentration and velocity microscales (*10*), λ_g, are related through the Schmidt number by $\lambda_\gamma^2 N_{Sc} = 2\lambda_g$.

Integrating Equation (2) with λ_γ^2 constant, we get

$$\overline{\gamma^2}(t) = \overline{\gamma^2}(0)\ \exp\ (-t/\tau)$$
$$\tau = \frac{\lambda_\gamma^2}{12D} = \frac{\lambda_g^2}{6D} \quad (4)$$

Corrsin applied these simplified concepts to an idealized turbulent mixer (*17*) and later extended the analysis (*18*) for arbitrary Schmidt number. One of the results was for the mixing time constant of Equation (4) to show that for $N_{Sc} >> 1$

$$\tau = \frac{1}{2}\left[4\left(\frac{L_\gamma^2}{\epsilon}\right)^{1/3} + \left(\frac{\nu}{\epsilon}\right)^{1/2} \log N_{Sc}\right] \quad (5)$$

where $L_\gamma = \int_0^\infty m(r)dr$ is the integral or macroscale (*10*), and ϵ is the turbulent energy dissipation rate per unit mass (*10*). Incorporated in this result for isotropic fields is the notion of Kolmogorov's universal equilibrium at large Reynolds numbers, as is evident from the Kolmogorov time scale $(\nu/\epsilon)^{1/2}$ in Equation (5).

Although experimental studies (*19, 7, 8*) for velocity, concentration, and temperature decay behind grids have been performed, the relatively low Reynolds number conditions were not suitable for proper test of the equations. Still, the minor effect of Schmidt number variation at large Schmidt number indicated in Equation (5) has been confirmed (*7, 8*). The data for grid generated fields have the form of

$$\overline{\gamma^2} = [\overline{\gamma^2}(0)] \propto (x/M)^a \quad (6)$$

independent of mean velocity. The results of this type of experiment have been discussed in some detail by Gibson and Schwarz (*7*).

The basic work on scalar mixing theory includes that of Batchelor (*20*) and Batchelor, Howells, and Townsend (*21*). Recent related studies include references *22* to *24*.

SOME PREVIOUS STUDIES OF CONCENTRATION FLUCTUATIONS

In 1959, Beek and Miller (*25*) presented some of the results of a numerical study of the mixing of miscible fluids in turbulent pipe flow. They found that the distance required to mix to a fluctuation variance of 1% of the initial value was roughly constant for gases over a wide range of Reynolds numbers, while the distance was greatly decreased for liquids with increasing N_{Re}. The results also show the decay of fluctuation variance with downstream position for tracer injection from various numbers of nozzles, N. Increasing N greatly increases the mixing of gases but was found to have a relatively minor effect on liquid mixing.

The details of the integration of the scalar spectrum equation employed in Beek and Miller's analysis are outlined in a survey article on mixing by Brodkey (*26*). Howells (*27*) developed a more general spectrum equation, and Lanza and Schwarz (*24*) present a numerical solution which shows good agreement with data.

Danckwerts (*28*), in an early paper on mixtures, proposed statistical measures to characterize the breakup and interdiffusion of two mutually soluble liquids. These are the scale and intensity of segregation. The scale of segregation is essentially the macroscale. The intensity of segregation I_s is a normalized concentration fluctuation variance defined as

$$I_s = \frac{\overline{\gamma_a^2}}{\overline{ab}} = \frac{\overline{\gamma_a^2}}{\overline{a}(1-\overline{a})} = \frac{\overline{\gamma_a^2}}{\overline{\gamma_a^2}_0} \qquad (7)$$

where the volume fractions of two liquids A and B at a point are a and b, with mean values of $\overline{a}$ and $\overline{b}$, and where $\overline{\gamma_a^2}_0$ is the initial variance. I_s is unity initially and, for complete segregation, will remain unity in the absence of molecular diffusion, while for a homogeneous (uniform) mixture, I_s is zero, as illustrated in (*26*).

In systems where mean concentration decays, the measured fluctuation decay includes the decay of mean concentration. Lee and Brodkey (*5*), in a study of turbulent mixing of dye injected into the core of a pipe flow, used I_s to recover the true intensity decay, that is, independent of mean concentration decay. I_s has the same form as the normalized fluctuation variance obtained from a solution for the decay in isotropic mixing as for Equation (4) and includes the volume ratio between the two components.

In turbulent diffusion in the core region of a turbulent pipe flow, the intensity is highest on the center line. Lee and Brodkey used this center-line decay as an upper limit for the whole pipe, although the calculated intensity must be readjusted to unity at the injector, and data must be smooth enough to allow this. In general, much care would be required for a meaningful application of I_s. For example, the dispersion results presented later in this paper could not be conveniently handled in this way.

Lee and Brodkey's measurements of I_s decay fell above the curve for low N_{Sc} time constant using Equation (4). However, with this time constant, $(L_\gamma^2/\epsilon)^{1/3}$ can be estimated (*5*) and used in Equation (5) to obtain the high N_{Sc} time constant, with the resulting curve above the data. The authors consider these curves bracketing the experimental points as good estimates of the mixing. Nevertheless, it must be remembered that dispersion in turbulent pipe flow involves far more, as indicated by Equation (1), than mere decay of variance by dissipation.

Experimental checks on variance behavior are strongly dependent on measurement methods and probe design. Lee and Brodkey developed and used a fiber optic light probe for their concentration measurements. Brodkey (*29, 30*) has modified and extended calculations originally presented (*5*). A later study with a smaller light probe (*31*) revealed that the intensity decay was significantly slower than shown in (*5*). However, comparison with other published results (*6*) and results obtained here indicates a lack of resolution of fluctuation variance even with this smaller light probe.

The turbulent dispersion of a tracer injected into the core of a turbulent pipe flow, often known simply as *turbulent diffusion*, has been treated in two ways other than by the direct application of simplified Eulerian statistical turbulence theory. The standard treatment employs Taylor's theory of "diffusion by continuous movements" discussed in detail in (*10, 32*). With this approach, for point source injection, if the mean concentration is normally distributed, measurements of the concentration half-radius, with distance from the origin, may be used to obtain the mean square material displacement from the center line, the velocity fluctuation intensity, and the eddy diffusivity.

A recent paper showing the results of this kind of approach has been presented by Becker, Rosensweig, and Gwozdz (*6*). For oil fog dispersion in air flow, they found relative intensities which were about six times as high as those obtained by Lee and Brodkey. Although different Schmidt number levels were involved, these results seem to indicate lack of resolution of the fiber optic probe.

Since for turbulent dispersion in the core of pipe flows, both the mean concentration and root-mean-square concentration fluctuation profiles are bell shaped and symmetric about the injection axis, Csanady (*33*) postulated a gradient diffusion relation for the flux of concentration variance in analogy to that for the turbulent concentration flux in terms of the eddy diffusivity. He replaced the rate of dissipation with the simplest consistent form $\overline{\gamma^2}/T(x)$, where $T(x)$ is an appropriate decay time scale depending on downstream position. With these changes and knowledge of the mean concentration field and eddy diffusivities, the simplified form of Equation (1) can be solved for $\overline{\gamma^2}$. With the eddy diffusivities for the turbulent concentration flux and flux of variance taken equal, the solution provides a good fit to the results of Becker et al. (*6*). Unfortunately, the simple self-similarity of profiles employed in the analysis is not generally found in more complicated flows like turbulent jets.

EXPERIMENTAL EQUIPMENT

A schematic diagram of the flow system used to prepare feed streams for the test section is shown in Figure 1. The 55-gal. drum was kept full with continuous overflow. Water was pumped from the drum bottom to the main flowmeter bank which consisted of two rotometers of maximum capacity of 2.5 and one of 9.6 gal./min.

Solutions of suitably high concentration of salt, dye, or reactants were pumped to the 13 gal. overhead carboys which were pressurized to 5 lb./sq.in. gauge to provide constant head for steady flow to the main water lines. Flow from overhead carboys was set with rotometers of maximum capacity of 20 gal./hr. This flow entered the main water line through a jet mixer. The combined concentrated feed and main water flow was then passed through a small mixing tank. This combination of initial mixing devices proved to be effective in delivering solutions of uniform composition to the test sections over the range of flow rates used.

Test Sections

The main water feed system was limited to about 5 gal./min., and, since duct Reynolds numbers of the order of 10^4 were required, test sections were necessarily small (about 4 sq.cm.). The test sections were of two different types.

1. A square duct of 3.72 sq.cm. area and 39 cm. long, made with glass sides and Lucite top and bottom. This duct was bolted to the feed and outlet sections with gaskets to keep the joints water and air tight. The duct was used in conjunction with two feed sections, as follows: two equal sized layers, 12 in. long, forming a flow hereafter referred to as a *plane mixing zone*, and a 3/16 in. layer ~10 in. long and fed with one solution, centered between two equal size layers, fed jointly with the other solution or water, forming a rough approximation to a plane ducted jet. These configurations are shown in Table 1 along with the initial velocities employed.

Feed sections were long enough for well-developed flow, and layers were separated by 1/64 in. stainless steel sheet sharpened at the test section entrance. The layer separators extended for about 1/8 in. into the square duct test section.

TABLE 1. FLOW CONFIGURATIONS AND INITIAL VELOCITIES

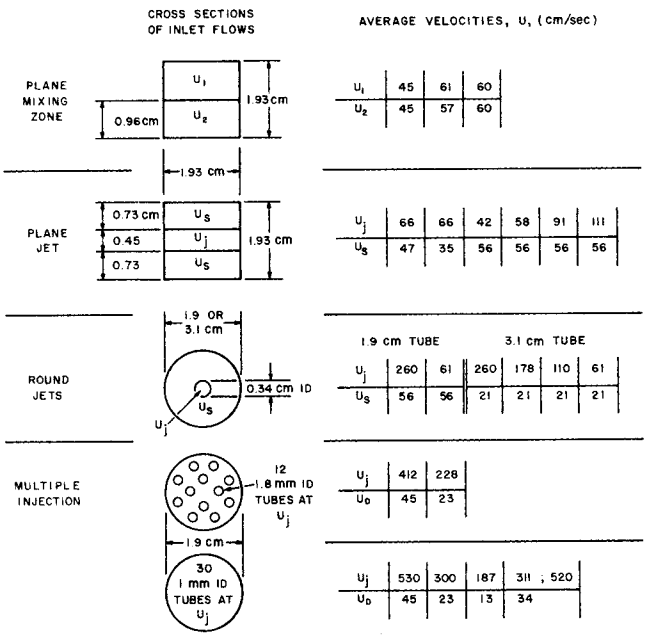

U_1	45	61	60				
U_2	45	57	60				
U_j	66	66	42	58	91	111	
U_s	47	35	56	56	56	56	
U_j	260	61	260	178	110	61	
U_s	56	56	21	21	21	21	
U_j	412	228					
U_o	45	23					
U_j	530	300	187	311 ; 520			
U_o	45	23	13	34			

Feed sections were smoothly joined to test sections with carefully cut gaskets to minimize disturbances.

Although the flows produced by these feed sections were far less than two-dimensional, near the origin in the vertical center plane, they did possess the essential properties of their ideal two-dimensional counterparts. Naturally, layer separators create velocity defects near the flow origin, and in square ducts these flows must eventually develop into turbulent duct flows. We must emphasize that our objective here was to compare the fluctuation intensity levels achieved and their downstream decay over a range of flow conditions. Disturbances to the velocity field at the point of injection, or contact between flow layers, and the lack of true two-dimensional flow undoubtedly influence the initial rate of mixing between the streams and properties like the jet potential core lengths. These disturbances would become important in careful studies of mean velocity or concentration decay as a function of flow conditions for ideal two-dimensional flows (for example, plane jets of high aspect ratio where development is not restricted by duct walls) but are of relatively minor concern here.

2. Standard Pyrex tubes were used for the preparation of axisymmetric ducted jet tubes and multiple injection systems. Single injectors of 3.4 mm. I.D. and 5 mm. O.D. were set along the axis of a 1.9 and a 3.1 cm I.D. tube. The injectors were 12 cm. long and tapered at the outlet. Disturbances caused by the wakes of jet feeder lines were not noticeable in dye tracer tests for turbulent jets. Finally, two 1.9 cm. I.D. tubes were prepared for multiple injection of two different

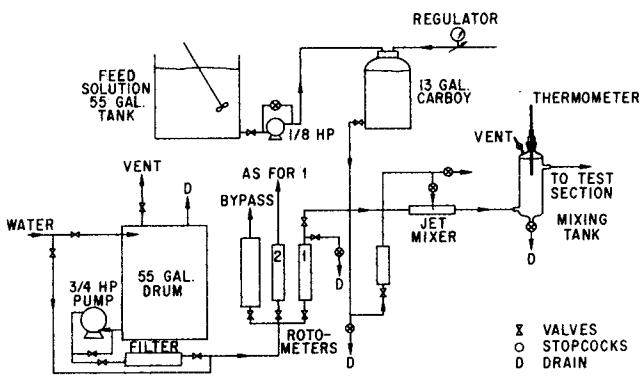

Fig. 1. A schematic of the flow system used for feed stream preparation.

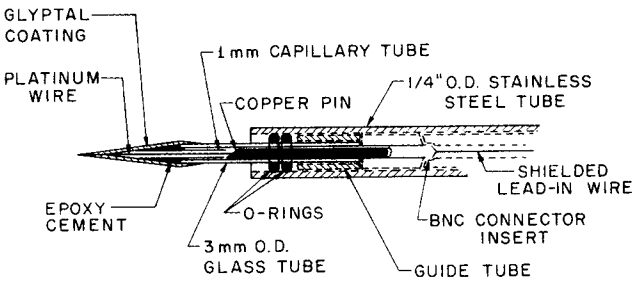

Fig. 2. A schematic diagram of the conductivity probe fitted into the positioning shaft.

solutions to allow for roughly uniform dispersal of one fluid in the other close to the point of injection. These tubes were similar in design to that used by Vassilatos and Toor (*34*). One tube contained twelve injectors of 1.8 mm. I.D. and the other thirty capillary injectors of about 1 mm. I.D. These configurations are shown in Table 1 along with the initial velocities employed.

The tubes were connected to the mixing tank lines with tapered adapter which matched the tube inside diameter and contained a calming tube bundle and grid. Even without the added disturbance of the jet injection tube, the turbulent flow in the main tube would not be well developed in the usual sense. However, jet characteristics dominated the field of interest, as will be evident from the results.

Probe positioning shafts of ¼ in. O.D. stainless steel passed through a ½ in. O.D. brass pivot ball machined for close fit with the ¼ in. shaft and mounted at the end of the outlet section to which test sections were secured with gaskets. O rings around the probe shaft on both sides of the pivot ball further secured the shaft and made the joint water tight. The shaft positioning device moved axially on two ¼ in. steel rods beyond the outlet section and was designed to allow for probe positioning at any point within the test section (*35*). It was most effective for use with axial positioning and probe movement in the vertical center plane of the various test sections. Cathetometer sightings of the probe to about 0.005 cm. were used for vertical positioning.

Probes and Measurement Technique

Microelectrodes were used to measure the point values of mean concentration and concentration fluctuations. The probe consisted of a tapered platinum wire encased in a tapered glass capillary and glyptal resin as shown in Figure 2. The cell constant [see for example (*7*)] for a typical probe was about 100 cm.$^{-1}$, and the sampling volume was on the order of 10^{-6} cc. Adequate resolution of fluctuation intensity was achieved by reducing the probe size until further size reduction did not change the measured intensity. The probe unit was set in the positioning shaft with O rings, and this arrangement simplified calibration procedures.

The circuitry employed in processing the fluctuating conductivity signal is shown schematically in Figure 3. The differential input gave a reduced noise to signal ratio of order 0.03%, the ability to measure relatively high level fluctuations, and a simple calibration compared with previous similar systems. The circuitry had flat frequency response to 6 kcp. with the halfpower point at 10 kcp. The signal was processed to obtain the time averaged mean value and the root-mean-square value of the fluctuations about the mean. Details on probe construction and electronic circuitry have been presented elsewhere (*35, 48*). Probe cell constants were determined with a Tektronix type Q transducer and strain gage plug in unit in conjunction with a Tektronix type 551 dual beam oscilloscope.

EXPERIMENTAL RESULTS

Concentration Fluctuations Associated with Mixing

In this section, measurements of mean concentrations

and root-mean-square concentration fluctuation intensities in various mixing systems are presented. Where possible and useful, results are compared with those of previous studies. The data presented here were obtained with microconductivity probes and dilute sodium chloride solutions in tap water. The available mixing theories, indicated previously, are appropriate only for relatively simple and more idealized systems than those considered here. Furthermore, because of the scope and diversity of the results presented, we have stressed the internal consistency of the results and the effects of varying flow conditions, rather than obscuring the results with some simplified and only partially useful mixing theory.

Multiple Injection

Decay of fluctuations on a constant background concentration in a flow of uniform velocity has received a fair amount of attention. In liquid systems, Gibson (*7*) injected salt solutions through a turbulence generating grid and measured spectra and fluctuation decay. Keeler (*8*) injected electrolytes through many hypodermic needles into a calmed uniform flow upstream of a turbulence generating grid such that mixing could be considered to begin at the grid. These systems are ideal in the sense that mean concentration is uniform across the section very close to the turbulence generating grids and that there is one-dimensional fluctuation decay downstream. Because uniformity of mean concentration (coarse scale uniformity) is achieved so rapidly, fluctuation intensity is fairly uniform across a section very close to the origin, and the intensity measured there may be used to normalize intensities at downstream positions.

Vassilatos and Toor (*34*) in an indirect verification of Toor's theory (*36*) for mixing and reaction measured conversion in a system designed to give rapid attainment of coarse scale uniformity. The device, which consisted of one hundred parallel tubes of 0.052 in. I.D. emptying into a 1.25 in. I.D. tube, served as the model for the multiple injectors used in this study. Their tube Reynolds number was 15,000, with the injection $N_{Re} = 3{,}700$. While recirculation can be expected to provide constant concentration across the section rapidly, it is clear that near the injectors the concentration field and distribution of fluctuation intensity will be quite nonuniform. For this kind of mixing device, then, there would be some practical difficulty in choosing the initial intensity for normalization of intensity decay and for subsequent application of turbulence theory results.

The intensity decay results for several multiple injection experiments are shown in Figure 4. Coarse scale uniformity was not established until about 3 or 4 cm. from the origin, precluding measurement of intensities near the origin. In particular, no data were taken closer than 1.5 cm. from the origin owing to wide variations there. The

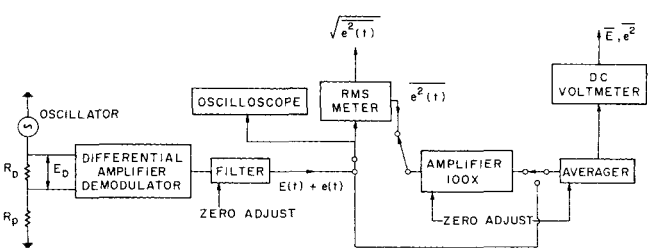

Fig. 3. Schematic diagram of differential input system and signal processing.

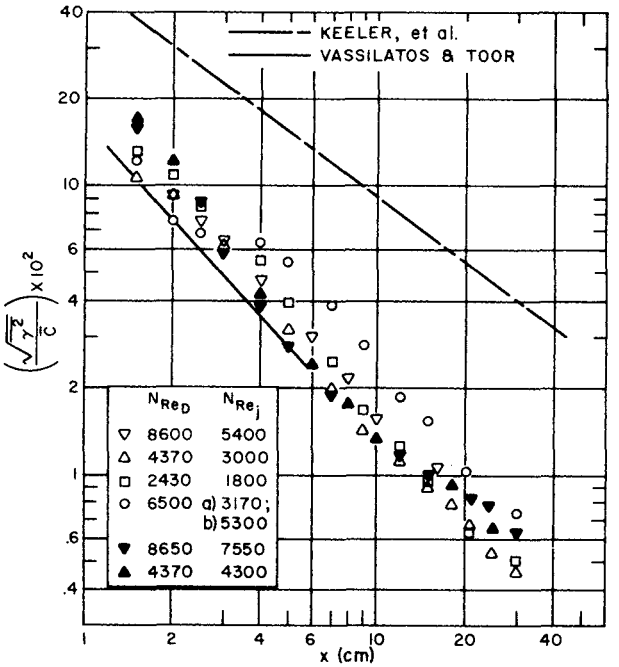

Fig. 4. Concentration fluctuation decay in 1.9-cm. I.D. tubes for multiple injection systems designed for rapid attainment of uniform mean concentration; ▽, △, □, ○—thirty 1-mm. I.D. injectors; ▼, ▲—twelve 1.8-mm. I.D. injectors.

decay is quite similar over a Reynolds number variation of a factor of 3 for matched injection velocities. Matched injection velocities occurred where only one jet Reynolds number is shown for the data symbols in Figure 4. The decay for one experiment with unmatched injection velocities is noticeably slower. Several experiments for five 1.7 mm. I.D. injectors in a 1.9-cm. tube for the same range of flow conditions gave similar but slower decay, and coarse scale uniformity was not reached until about 8 cm.

The results of Vassilatos and Toor (*34*) for $N_{Re_D} = 15{,}000$ and of Keeler et al. (*8*) are also shown on Figure 4. It appears that for similar flow systems, the doubling of N_{Re_D} over the maximum for the present experiments has little effect on increasing fluctuation decay. Keeler's experiments in grid generated turbulence employed mesh lengths of ¼ in. in 2-in. tubes with mesh Reynolds numbers of 800 to 2,400. Keeler's results are consistent with an exponent in Equation (6) of $a = -1.5$ in agreement with idealized theory (*10*). Furthermore, Keeler found that $\sqrt{\overline{\gamma_0^2}} \cong \overline{C}$. This condition is implied in the presentation of Vassilatos and Toor's results, which are in turn inferred from reaction studies via Toor's theoretical relation for the equivalence of fractional conversion and unaccomplished mixing.

The striking similarity of intensity decay for multiple injection systems over a range of Reynolds numbers is encouraging and suggests a wider qualitative applicability for Toor's theory than may have been anticipated.

Round Turbulent Jets

The work on scalar fluctuations in round turbulent jets far exceeds similar studies for any other free shear flow. Rosensweig (*1*) developed and used the smoke-scattered light technique to obtain concentration fluctuation intensities and related turbulence results for a jet Reynolds number, $N_{Re_j} = 20{,}200$. His thesis also contains some preliminary results for a ducted jet. Becker used the same technique (*37*) to obtain extensive measurements of the concentration fields and other turbulence characteristics

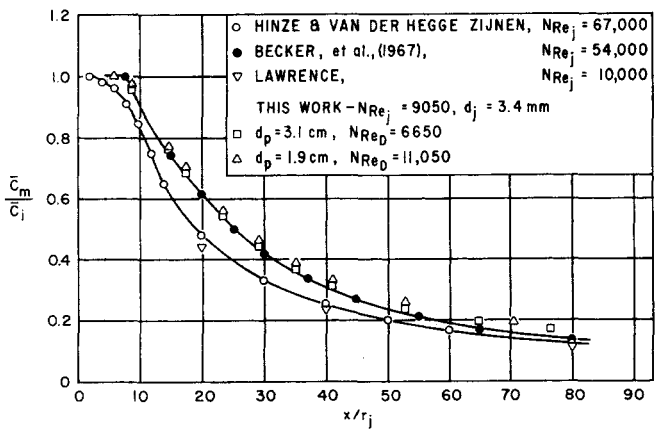

Fig. 5. Center line mean concentration decay for round turbulent jets. For this work $\overline{U_j}$ = 260 cm./sec. and □—$\overline{U_s}$ = 21 cm./sec. △—$\overline{U_s}$ = 56 cm./sec.

in a ducted jet mixing with varying degrees of recirculation. These results include those for mean velocity and concentration fields (*38*), the concentration intermittency (*39*), and concentration fluctuations and turbulence characteristics (*3*). Becker et al. (*4*) also obtained detailed results for a free turbulent jet with N_{Re_j} = 54,000 and presented a comparison with similar studies by others.

Wilson and Danckwerts (*2*) measured temperature fluctuations in a hot air jet with N_{Re_j} = 2 to 4 × 10^4, and several similar studies have been made. However, the only measurements for concentration fluctuations in free turbulent liquid jets seem to be those of Lawrence (*40*) who used conductivity probes for N_{Re_j} = 1 to 2 × 10^4.

The results for round turbulent jets presented here were obtained in the course of several experiments on the effect of jet Reynolds number on the nature of the concentration fluctuation intensity in ducted jet and injection mixing in a turbulent pipe flow.

The center-line mean concentration decay for round turbulent jets is presented in Figure 5, where N_{Re_j} = 9,050 in each case. While this value is lower than that usually employed, the mean decay is consistent with more fully developed jets, and the basic turbulent jet characteristics are observed.

The center-line decay of mean concentration in the 3.1-cm. tube, for which the (secondary) pipe flow velocity is only about 21 cm./sec., follows Becker's results (*4*) for a well-developed free turbulent jet, given by

$$\overline{C_i}/\overline{C_m} = 0.185\,[(x/d_j) - 2.4]$$

for $(x/d_j) \geq 20$ and plotted for comparison in Figure 5. $\overline{C_i}$ is nozzle concentration, $\overline{C_m}$ is center-line concentration, x is axial position, and d_j is the injector diameter. Downstream, the present results are consistently above Becker's, reflecting the fact that mean concentration must eventually decay more slowly for ducted jets because of confining walls. Values of $\overline{C_m}/\overline{C_i}$ in the 1.9-cm. tube are similar and somewhat above the others because of the smaller confining tube and higher secondary velocity, which also decreases the extent of decay at a given position.

More rapid decay of center-line concentration was obtained by Lawrence (*40*) in free salt solution jets formed with short radius nozzles of 1/8, 3/16, and 1/4 in. diameter for N_{Re_j} = 10^4, 12,800, and 19,200. His results for N_{Re_j} = 1/8 in. are included in Figure 5, but the decay was nearly the same for every nozzle over the Reynolds number range he studied.

Many studies of heat and mass transfer (that is, mean property profiles) in free turbulent jets have been made, and significant differences between results of various studies under apparently similar conditions often occur. Becker et al. (*4*) list and comment briefly on many of these results. Hinze and Van der Hegge Zijnen (*42*) employed 1% town gas in an air jet with N_{Re_j} = 67,000 and d_j = 2.5 cm. Their normalized center-line decay, also shown in Figure 5, was similar to Lawrence's results. In these studies, the jets emanated from thin orifices at the end of a tube of much larger area. The differences in the center-line decay curves reflect different nozzle designs, although other factors such as sampling methods and the nature of the probe measuring system could contribute. In any event, Becker's rather complete results provide the best yardstick for comparison with other work.

The center-line relative intensities of concentration fluctuations in round turbulent jets are presented in Figure 6, as are the data of other studies. Becker's results (*4*) best reflect well-developed turbulent jet characteristics. He states that the first maximum indicates that the basic jet structure has been formed but is not yet in equilibrium. Rosensweig's data [estimated from Figure 7 of (*1*)] are for N_{Re_j} of only half that used by Becker, but both studies used ideal flow nozzles to obtain initially flat velocity profiles. In each case, the relative intensity reaches about 21%.

In view of the differences in the jet Reynolds numbers and the initial conditions for the jet in the 3.1-cm. tube when compared with those for the others shown, the relative intensity behavior is surprisingly similar and reaches 19% before decreasing owing to slowed mean concentration decay in the small diameter tube. Results in the 1.9-cm. tube (see Figure 8) were similar, but the maximum relative intensity was somewhat lower due to the higher velocity secondary tube flow and confined mean decay.

Lawrence's results (*40*) for relative intensities were a good deal higher than those of Figure 6, ranging between 24 and 30% at x/d_j = 40. For N_{Re_j} = 10^4 and d_j = 1/8 in., the center-line relative intensities were 13, 21, and 27% at x/d_j = 10, 20, and 40, respectively, and those results were roughly intermediate to those for all of Lawrence's flow conditions. His relative intensities generally increased as Reynolds numbers decreased, and a nozzle size effect for a given Reynolds number was observed. Lawrence's high relative intensity results are probably in part a consequence of the particular nozzle configuration. However, internal inconsistencies and the use of relatively large conductivity probes, with cell con-

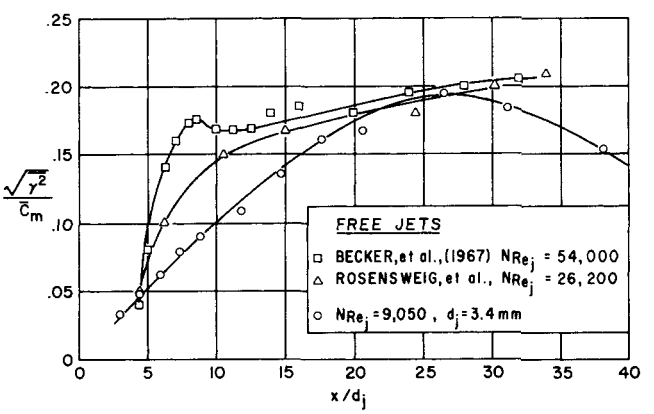

Fig. 6. Center line relative concentration fluctuation intensities for round turbulent jets. For this work ○—d_p = 3.1 cm., $\overline{U_j}$ = 260 cm./sec., $\overline{U_s}$ = 21 cm./sec., and N_{Re_D} = 6,650.

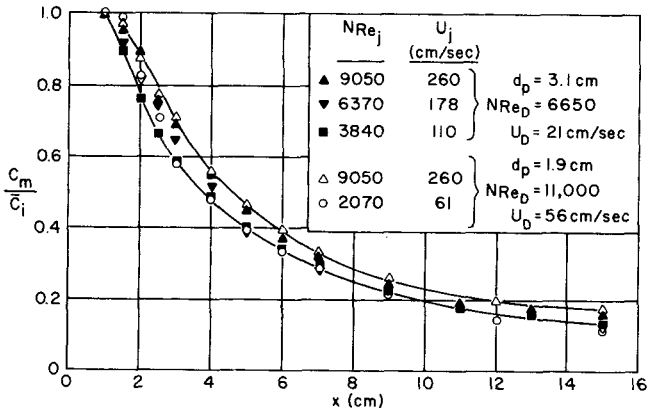

Fig. 7. Center line mean concentration decay for jet injection into a turbulent pipe flow, d_j = 3.4 mm.

stants of about 40 cm.$^{-1}$, cause some doubt as to the precise values of the numerical results. The probes certainly lacked the required resolution to record true point values of fluctuation intensity, since in the present experiments for similar flow conditions, probes with cell constants of 60 cm.$^{-1}$ showed a consistent lack of resolution when compared with results obtained with probes of cell constants of 80 cm.$^{-1}$ or more. From a simple model (for example, 7), probes with cell constants of 40 cm.$^{-1}$ sample a volume an order of magnitude larger than that for probes with cell constants of 80 cm.$^{-1}$ Comparison of Lawrence's intensities normalized with the initial mean concentration, to minimize the effect of his more rapid center-line mean concentration decay, shows that the results are consistently lower than those for the other free jets (Figure 6).

Dispersion in Turbulent Pipe Flow

Most studies of tracer dispersion in the core of turbulent pipe flows determined eddy diffusivities and turbulence intensities from measured mean concentration profiles. Lee and Brodkey (5) obtained the first results for concentration fluctuation intensity for dye tracer dispersion in such flows. They employed a ¼-in. injection tube centered in a flow of N_{ReD} = 50,000 in a 3.068 in. I.D. pipe, and the injection velocity was chosen to minimize the disturbance to the subsequent pipe flow velocity profile.

Their apparent center-line relative intensity rose to a plateau of about 16% at 24 in. from the injector and fell more slowly from about 48 in. downstream. Their fiber optic light probe had a gap of about 1 mm. and sampled a volume of 5.6 × 10^{-4} cc. More recent center-line measurements of intensities by Nye and Brodkey (31) for the same flow conditions were made with an improved light probe sampling about 1.2 × 10^{-5} cc. with a gap of 0.25 mm. From their plot of intensity of segregation (I_s) decay, it is clear that Lee and Brodkey's original results fell well below the new data, confirming the significant lack of resolution with the original probe. When these I_s decay curves are used to correct Lee and Brodkey's center-line relative intensity results, it is found that the corrected relative intensity now reaches a plateau of about 20%, and the length of this plateau is extended to about 72 in. downstream.

Becker, Rosensweig, and Gwozdz (6) injected oil fog tracer from 2.16 mm. I.D. tubing into well-developed flows in 8-in. diameter pipe for several Reynolds numbers on the order of 5 × 10^5. They matched the injection velocity to the local mean pipe flow velocity and used the scattered light technique (37) for measurements of concentration fields. Center-line relative intensities were found to be about 100% for downstream positions of from 1 to 5.6 pipe diam. These results were about six times as high as the 16% intensities obtained by Lee and Brodkey, whose low readings can probably be attributed largely to limited resolution of the fiber optic light probes.

The tubes used in the present study for turbulent jet measurements were also used for some measurements of center-line mean concentration and fluctuation intensity as the injection velocity was decreased, thereby approaching conditions for pipe flow dispersion. Data for center-line mean concentration decay are shown in Figure 7, with turbulent jet results included for comparison. The decay is slowest for the most turbulent jet, with N_{Re_j} = 9,050, and becomes faster as the injection Reynolds number is decreased.

Center-line relative intensity curves are shown in Figure 8 for a range of flow conditions. They are bounded below by results for the turbulent jets. As N_{Re_j} is decreased, the intensities rise, reflecting the change in mixing characteristics from that of turbulent jets to systems in which the pipe flow has ever-increasing effect. For the 3.1-cm. tube, at the lowest N_{Re_j} = 2,070, the curve peaks at 57%, although the injection velocity was still three times that of the pipe flow. The highest intensity of about 68% was

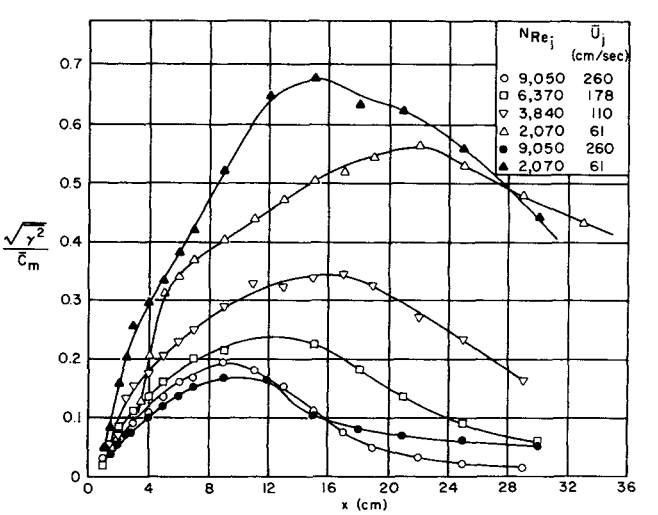

Fig. 8. Center line relative intensities for jet injection at various jet Reynolds numbers. Mean concentration decay is shown in Figure 7, and ○, □, ▽, △—d_p = 3.1 cm., N_{ReD} = 6,650, ●, ▲—d_p = 1.9 cm., N_{ReD} = 11,000.

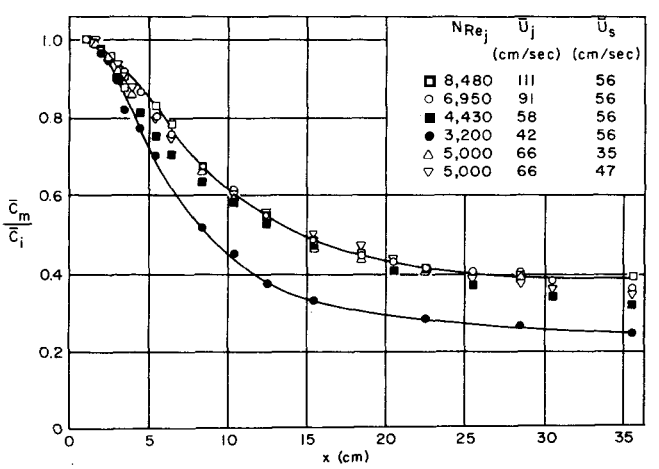

Fig. 9. Center line mean concentration decay in the plane jet for a range of flow conditions.

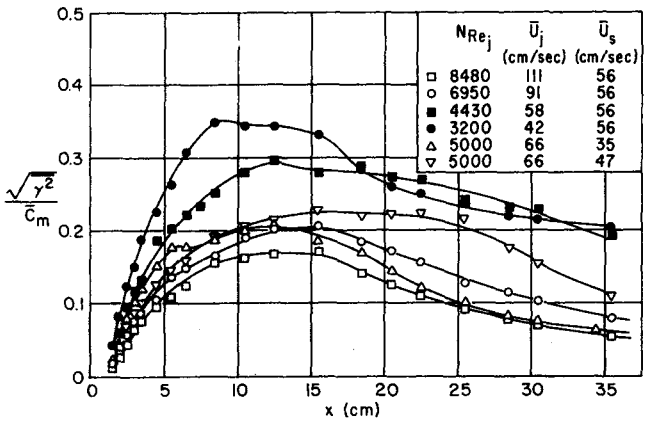

Fig. 10. Center line relative intensities in the plane jet for a range of flow conditions, with mean concentration decay shown in Figure 9.

obtained in the 1.9-cm. tube for which $N_{Re_j} = 2{,}070$, and injection and pipe flow velocity were nearly matched. These last results come closest to dispersion in turbulent pipe flow, and, but for the confining effects of the small pipe, it seems clear that these intensity curves would have continued to rise, in at least qualitative agreement with the 100% relative intensity levels measured by Becker et al. for their oil fog dispersion in air.

Plane Ducted Jet

The plane jet used in this work, emerging from a slot with the very low aspect ratio of about 4 to 1, was rather far removed from the true two-dimensional jets used in turbulence studies. However, the intensity profiles close to the origin exhibited the characteristics that would be observed in more ideal jets. The jet Reynolds number is specified in terms of the slot hydraulic diameter of 7.3 mm., rather than the usual slot width (here 4.5 mm.).

Results for center-line mean concentration decay are shown in Figure 9 for a range of jet and secondary ($\overline{U}_s$) velocities. The decay is slower for these low aspect ratio jets than for free fully developed turbulent plane jets (for example, *44*). The confining effects of the secondary flow would also be pronounced for these jets. Forstall and Shapiro's results (*41*) for a round turbulent jet in a pipe flow indicate that when $\overline{U}_s/\overline{U}_j$ increases from 0 to 0.5, then $\overline{C}_m/\overline{C}_i$ nearly doubles at $x/d_j = 20$. In further similarity to round jets, the decay is slowest for the greatest N_{Re_j}, and there is consistent increase as the jet Reynolds number decreases. The flow for the lowest injection Reynolds number of 3,200 is closest to the case of dispersion in turbulent duct flow, and it exhibits the most rapid center-line decay. The decay should be slowed by the horizontal duct walls at about 8 to 10 cm., and this effect is evident in Figure 10.

Relative intensities of center-line concentration fluctuations for a variety of flow conditions are presented in Figure 10. The results show the same general trends as those for injection from a round tube. The relative intensity curve for the most turbulent jet, $N_{Re_j} = 8{,}500$, forms a lower bound for all other results and reaches about 17%. The curve for the lowest injection velocity, with $N_{Re_j} = 3{,}200$, peaks at about 35%. The relative intensities are lower than results for the round jets, owing to the decreased length of unimpeded spread and also a more restricted range of flow conditions. Further downstream, the relative intensities fall at various rates due to complex interactions between Reynolds numbers, initial concentration levels, and the ratio of injection to secondary velocities.

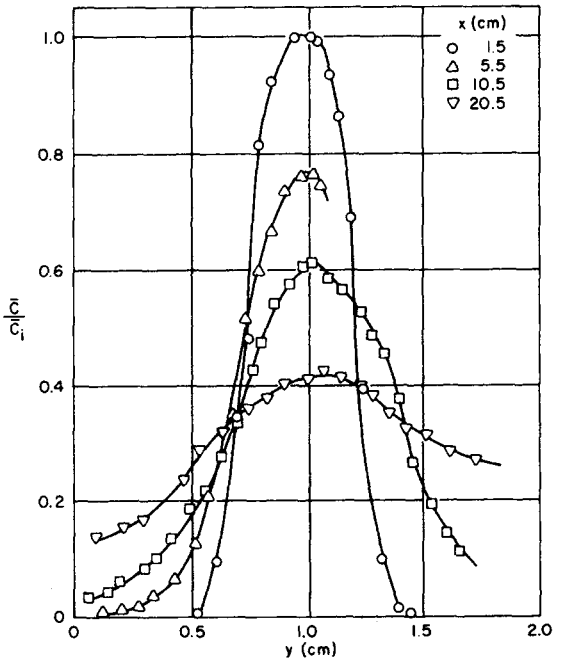

Fig. 11. Mean concentration profiles for the plane jet with $N_{Re_j} = 5{,}000$, $\overline{U}_j = 66$ cm./sec., $\overline{U}_s = 47$ cm./sec.

Profiles for mean concentration and the corresponding relative intensities are presented in Figures 11 and 12 for $N_{Re_j} = 5{,}000$. Mean concentrations have been normalized with the injection concentration, while intensities are divided by the center-line or maximum mean concentration at the same axial position. The lack of symmetry evident for $y > 1$ cm., and increasing with downstream position reflects somewhat unequal velocities in the upper and lower flows and slight misalignment between feed

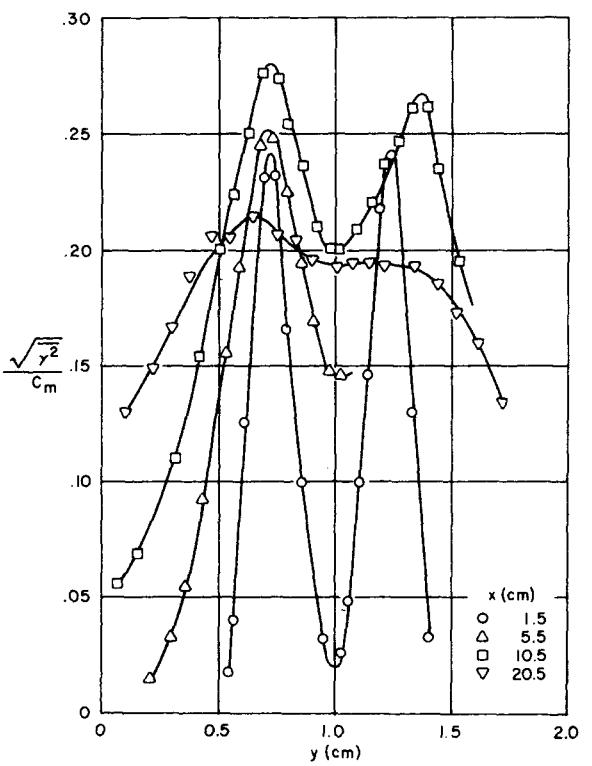

Fig. 12. Relative intensity profiles for the plane jet as per Figure 11.

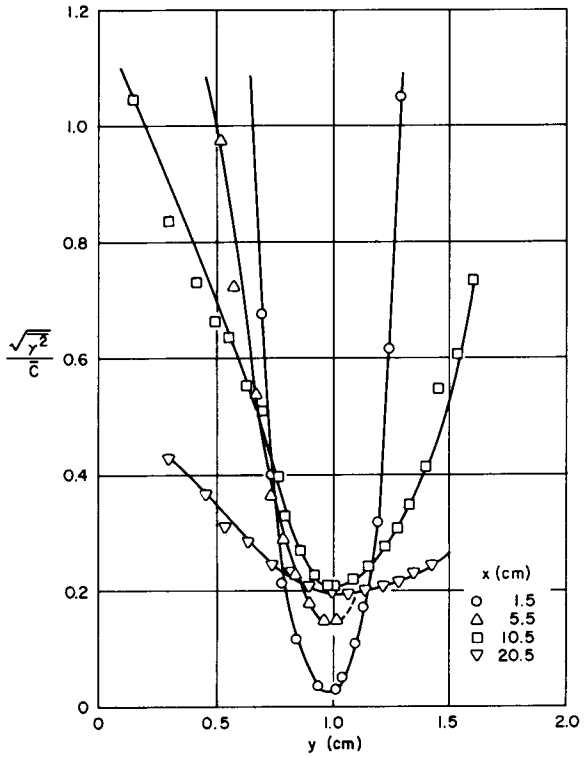

Fig. 13. Relative intensity profiles for the plane jet based on local mean concentration, from Figures 11 and 12.

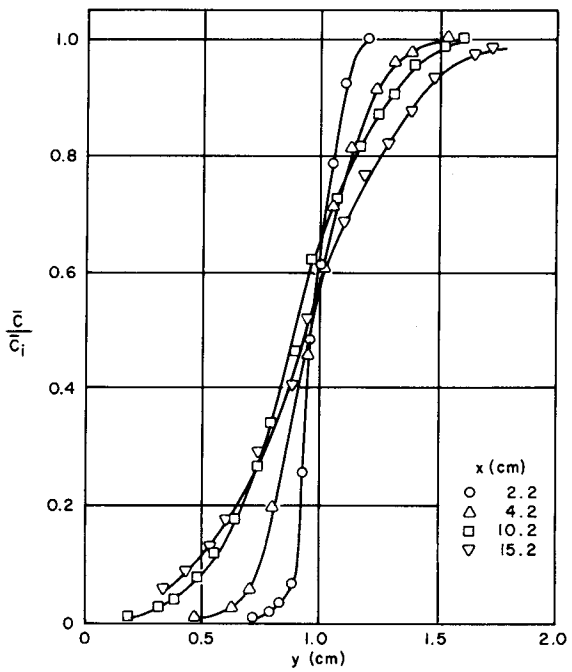

Fig. 14. Mean concentration profiles for the mixing zone with $N_{ReD} = 8{,}400$, $\overline{U_1} = \overline{U_2} \cong 45$ cm./sec.

and test sections. These effects are not great and are of little consequence here.

The relative intensity in Figure 12 for $x = 1.5$ cm. falls to nearly 0 at the center line since the jet potential core ends at about this position. The relative intensity minima on the center line, characteristic of turbulent jets, is clearly observed. Jet fluid reaches the horizontal duct walls by $x = 10$ cm., and by $x = 20.5$ cm. the intensity profile has undergone a good deal of leveling in the central part of the duct. Townsend's concept (9) of the double structure of free shear flows may be made the basis of a model to fit the observed double peaked intensity profiles in free jets. Here the nonideality of the plane jets and the relatively short length of unimpeded flow development would obscure any such attempts.

Results for relative intensities based on local mean concentration for the experimental conditions of Figure 12 are shown in Figure 13. At the high relative intensities so obtained in the outer mixing region of the jet, errors due to long averaging times and small mean signals become troublesome.

Pulse count profiles (35) for $N_{Rej} = 5{,}000$ look like the relative intensity profile of Figure 12 at $x = 1.5$ cm., since there are few fluctuations near the tip of the jet potential core. Further downstream, the pulse count is constant across the central part of the jet, since fully turbulent jet fluid occurs there. The pulse count falls off in the intermittent region, and its general behavior is similar to that of the intermittency factor (39). By using these data, the concentration microscale may be estimated to be about 0.07 cm. and is therefore larger, by a factor of 100, than the equivalent radius of the microconductivity probe of cell constant 100 cm.$^{-1}$

With $N_{Rej} = 4{,}500$ and jet and secondary velocities matched at 57 cm./sec., the relative intensity at $x = 20$ cm. was still at 25% rather than falling to about 20% as in Figure 12, and the central minima were not as low. However, for $N_{Rej} = 7{,}000$, in a secondary of 56 cm./sec., the relative intensity maxima are somewhat lower than that shown in Figure 12, although basically similar.

Plane Mixing Zone

A plane mixing zone was formed by joining two developed flows, emerging from slots of 9.6 mm. width, in the square duct of 1.93-cm. sides. The confining duct soon distorted the mixing zone, and true symmetry was lacking. These flows will be specified by the velocities in the upper ($\overline{U_1}$) and lower ($\overline{U_2}$) layers and the Reynolds number for the duct based on the total flow.

Profiles of mean concentration and relative intensities normalized with the initial concentration are shown in Figures 14 and 15 for matched velocities and $N_{ReD} = 8{,}400$. The relative intensity curves are steep and narrow near the origin and peak at lower values as they spread downstream. As with turbulent jets, the relative intensity peaks occur at the half-concentration position. Pulse count profiles for this flow show that at downstream positions the core of the mixing zone is essentially fully turbulent but not free of some intermittency, as was the case for turbulent jets. The concentration microscale is about 1 mm.

The profiles in Figures 14 and 15 were obtained with a probe of cell constant of 80 cm.$^{-1}$. The relative intensity curve for 2.2 cm. peaks at 29%. Under the same flow conditions, when a probe of cell constant 40 cm.$^{-1}$ was used, the relative intensity peak at 2.2 cm. was 26%. Although this lack of resolution with the larger probe was not excessive, it was consistently observed when larger probes were used. Hence, fluctuation measurements in this work were obtained with probes of cell constants of 80 to 120 cm.$^{-1}$.

The fiber optic light probe built for this study gave a relative intensity of only 25% at $x = 2.2$ cm. Since the gap was 0.7 mm., the true intensity peak with its sharp curvature over a similar length scale could not be properly resolved. Corrections for background noise, drift, and the nonlinear relation between voltage and concentration made accurate light probe measurements difficult, irrespective of the probe resolution, and the light probe was soon discarded.

With unmatched initial velocities, $\overline{U_1}$ = 45 cm./sec., $\overline{U_2}$ = 67 cm./sec., and N_{Re_j} = 9,250, the relative intensities peaked well below those in Figure 15, and the half-concentration positions moved into the upper layer with increased downstream position due to the more rapid lower water layer. Relative intensity profiles for N_{Re_D} = 6,400 and nearly matched velocities were similar to those of Figure 15, but the peak values fell more slowly with increased axial position.

Profiles for N_{Re_D} = 11,800 and nearly matched velocities are shown in Figures 16 and 17. The relative intensities for this flow peak at lower values than those for the lower Reynolds number flow are shown in Figure 15. Intensities normalized with local mean concentrations for the results of Figures 16 and 17 are shown in Figure 18. These relative intensities rise rapidly in the tracer free water layer. Oscilloscope traces corresponding to the results shown in Figure 17 clearly reveal the highly intermittent character of the mixing zone (35). The smallest wrinkles on the traces corresponded to eddy sizes of about 0.15 mm.

CHEMICAL REACTIONS IN TURBULENT FLOWS

Apparently the only comparison of concentration fluctuation decay in liquid mixing and conversion in the equivalent reacting system is that of Keeler et al. (8). His system in which the mixing and reaction could be considered to begin at the turbulence generating grid provided a relatively ideal situation in which to test Toor's reaction model (36). Several recent studies (45, 46) obtained time exposure photographs of colored reaction zones, but quantitative results are difficult to deduce from such experiments.

In this work, the very rapid irreversible reaction, used by Keeler, of acetic acid and ammonium hydroxide in dilute solutions to give a highly conductive reaction product solution was employed to obtain mean product concentrations for multiple injection, the plane jet, and the mixing zone.

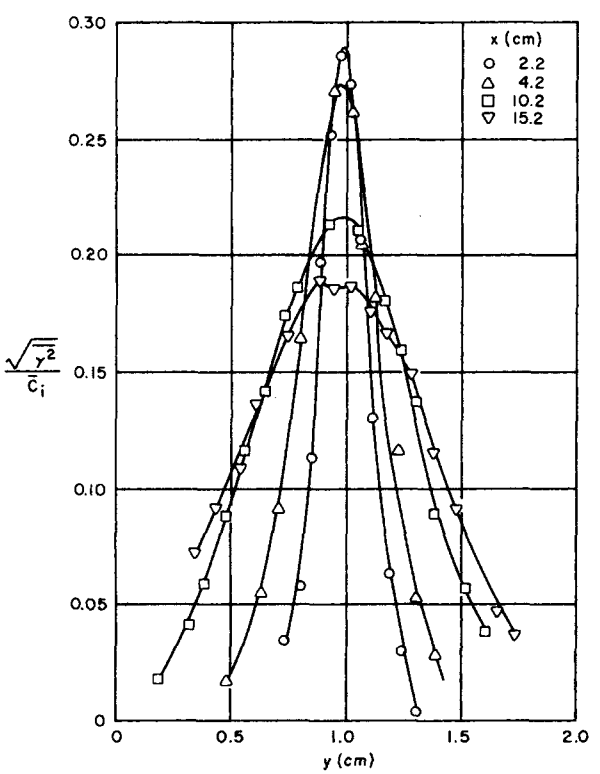

Fig. 15. Relative intensity profiles for the mixing zone for the conditions of Figure 14.

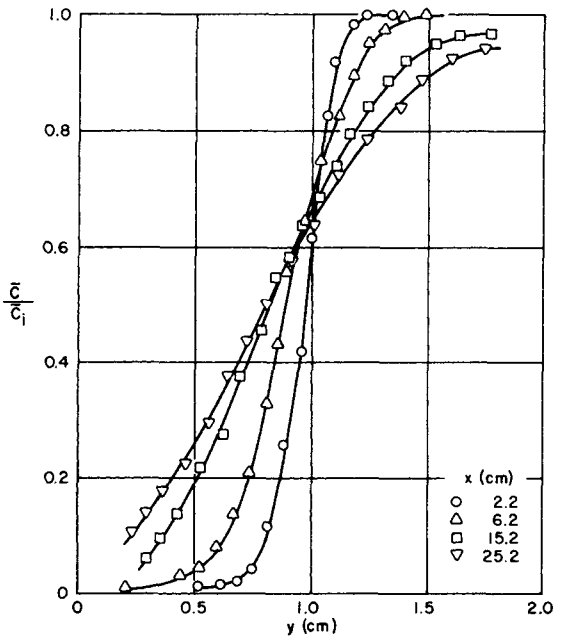

Fig. 16. Mean concentration profiles for the mixing zone with N_{Re_D} = 11,800, $\overline{U_1}$ = 61 cm./sec., $\overline{U_2}$ = 57 cm./sec.

Multiple Injection

According to Toor's very rapid reaction model, the accomplished mixing, that is, $[1 - (\sqrt{\overline{\gamma^2}}/\sqrt{\overline{\gamma_0^2}})]$, should be equal to the fractional conversion for stoichiometric mixtures in systems in which conditions at the plane of coarse scale uniformity have been used for normalization. It was noted above that for a multiple injection system, where intense recirculation at the origin is required to obtain

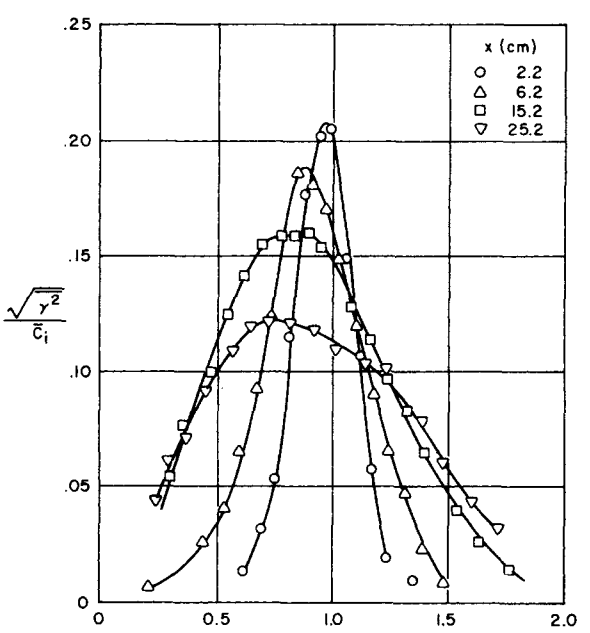

Fig. 17. Relative intensity profiles for the mixing zone for the conditions of Figure 16.

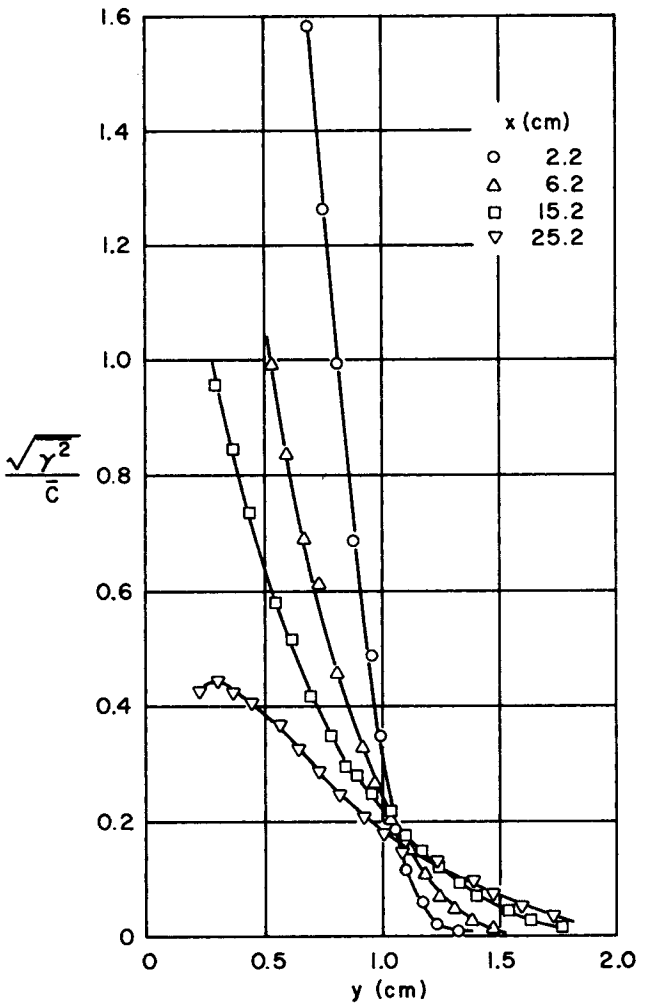

Fig. 18. Relative intensity profiles for the mixing zone based on local mean concentration for the conditions of Figures 16 and 17.

mean concentration uniformity in that region, considerable reaction will have occurred before the condition of uniformity is reached. This fact makes the choice of an initial mean square intensity practically impossible. Vassilatos and Toor (34) verified the model indirectly by measuring only conversion for various ratios of initial reactants concentrations and comparing the results with those for a stoichiometric ratio of reactants. Keeler was able to take the origin of the mixing and reaction at the turbulence generating grid. Since the turbulence was relatively weak, an appreciable distance in the test section was required for complete reaction, and measurements were in agreement with Toor's model.

Concentration fluctuation decay for mixing from multiple injection systems has been presented in Figure 4. Reaction studies carried out in the same equipment for the condition of $N_{Rej} = 5{,}400$ and $N_{ReD} = 8{,}600$ show that the fractional conversion curve was indeed the mirror image of the accomplished mixing curve, where initial intensity was replaced by mean concentration. Coarse scale uniformity was attained at about 4 cm., although reasonable concentration estimates were possible at 2 cm. from the origin. Since at 2 cm. the reaction was nearly 90% complete, it was obviously difficult to apply Toor's model quantitatively. For comparison, Vassilatos and Toor obtained 90% conversion at 0.625 in. with $N_{ReD} = 15{,}000$. Keeler found about 70% conversion at 10 cm. These numbers may be estimated from the mixing results of Figure 4 as $[1 - (\sqrt{\overline{\gamma^2}}/\bar{C})]$.

Plane Ducted Jet

System output profiles for reaction in the plane jet for $N_{Rej} = 7{,}000$ and equal initial concentrations (that is, $\beta = 1$) of the acetic acid jet and ammonium hydroxide secondary are shown in Figure 19. The stoichiometric parameter β is the ratio of initial reactant concentrations. Nearest to the origin, at $x = 2$ and 5.5 cm., the peaks are at about the same position at the relative intensity peaks for mixing without reaction for the same flow conditions.

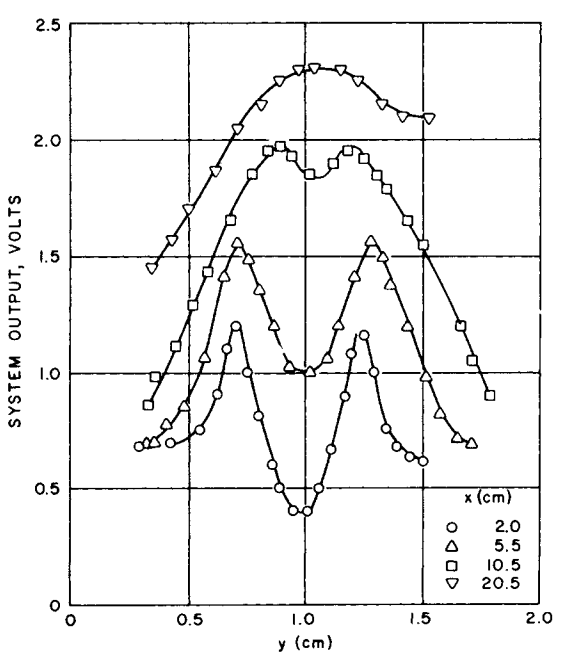

Fig. 19. Profiles of output voltage for reaction in the plane jet for $N_{Rej} = 7{,}000$, $\overline{U_j} = 91$ cm./sec., $\overline{U_s} = 56$ cm./sec., and $\beta = 1$.

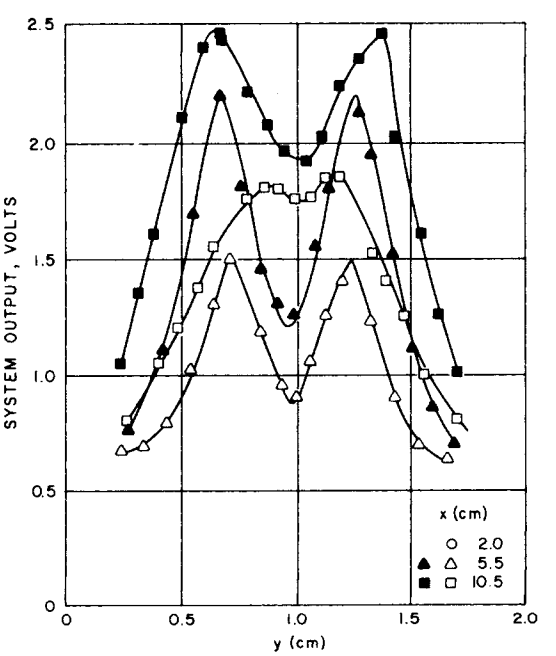

Fig. 20. Profiles of output voltage for reaction in the plane jet for $N_{Rej} = 4{,}500$, $\overline{U_j} \cong \overline{U_s} = 57$ cm./sec., △, □ — $\beta = 1$; ▲, ■ — $\beta = 2$.

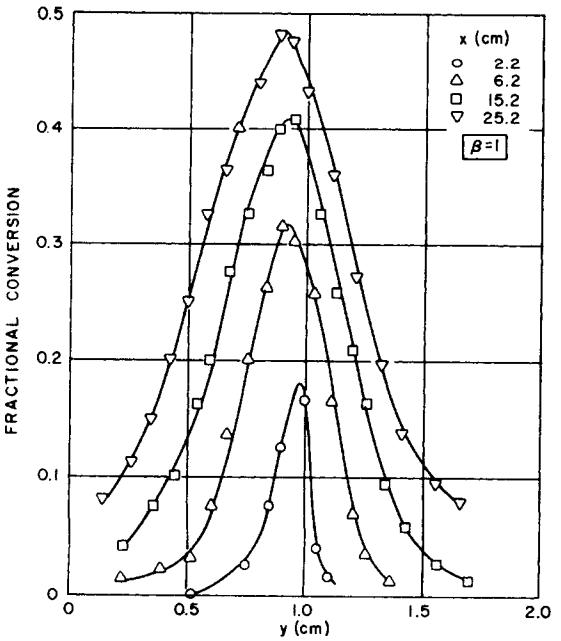

Fig. 21. Fractional conversion profiles for the mixing zone with $N_{ReD} = 13{,}000$, $\overline{U_1} \cong \overline{U_2} = 60$ cm./sec., with $\beta = 1$.

Further downstream, the peaks are reduced in size and shifted closer to the center line as the reaction works its way into the jet core. By $x = 20.5$ cm., the concentration is highest on the axis. The asymmetry evident in the upper portion of the flow reflects the fact that the upper secondary flow is less than the lower.

The system output shown in Figures 19 and 20 includes contributions from unreacted acid and base. Corrections to recover the reaction product concentration are difficult for this kind of flow, but the profiles shown well illustrate the nature of the product concentration profiles. The jet and secondary did not have equal flow rates in Figure 19, and ultimate product concentration after complete conversion in a well-mixed system would correspond to about 2.15 V.

In Figure 20, with $N_{ReD} = 4{,}500$, closest to the origin at $x = 5.5$ cm., the peaks occur at the same position as the relative intensity peaks for tracer mixing under the same flow conditions. At $x = 10.5$ cm., the peaks are reduced in size and are closer to the jet center line for $\beta = 1$.

For Figure 20, the ultimate concentrations after complete conversion in a well-mixed system would correspond to about 1.4 V. for $\beta = 1$ and about 3.2 V. for $\beta = 2$. Hence, conversion in this jet is less than that in the more turbulent jet with $N_{Rej} = 7{,}000$. This result is in accord with the reduced fluctuation intensity in mixing systems as the jet Reynolds number is increased. From Figure 20, when the initial concentration of the acid jet is made twice that of the basic secondary, the peaks in product concentration are significantly increased, as is the general level of local conversion. There is also a noticeable shift of the peak position in the more dilute basic secondary flow.

Plane Mixing Zone

Fractional conversion profiles, which were estimated from system output corrected for the contributions of reactants, for the mixing zone with $N_{ReD} = 13{,}000$ and $\overline{U_1} \cong \overline{U_2}$ are shown in Figures 21 and 22. The stoichiometric parameter β is seen to have a significant effect on conversion. In fact, the ratio of peak fractional conversion for $\beta = 1$ to that for $\beta = 2$ is about 0.66 for each axial position. Also, for $\beta = 2$, the curves clearly shift into the more dilute lower layer with increasing downstream position.

Fractional conversion profiles for the mixing zone with $N_{ReD} = 6{,}750$ and $\overline{U_1} \cong \overline{U_2}$ exhibited the same general behavior as did those of Figures 21 and 22. For this case, the ratio $F(\beta = 1)/F(\beta = 2)$ for peak conversion is about 0.75 for each axial position.

From these results, increasing β above unity is more effective in increasing the fractional conversion at higher Reynolds numbers, that is, in more fully developed free turbulent flows. Furthermore, the larger peak conversions in the flow of larger Reynolds number are consistent with the smaller relative intensity levels in the equivalent mixing systems at larger Reynolds number.

When the profile widths at a conversion of half the maximum are compared, the widths for $N_{ReD} = 6{,}750$ are significantly larger at $x = 15$ cm. than those for $N_{ReD} = 13{,}000$, illustrating the effect of the different flow fields. The results for larger Reynolds number would tend to exhibit in larger measure the characteristics of a developed free mixing zone. At lower Reynolds number, the larger scale components of duct flow become more important.

SUMMARY

Measurements of the relative intensities of center-line concentration fluctuations for injection into turbulent pipe flow show that decreasing the injection Reynolds number from that characteristic of turbulent free jets to that causing minimum disturbance to the pipe flow profile causes the relative intensities to increase between the limits set by turbulent jets of about 20%, up to about 68% in the present experiments. These results support the relative intensities of 100% obtained by Becker et al. for dispersion in pipe flow under more ideal conditions. Lee and Brodkey's data, obtained with a fiber optic light probe of relatively large sampling volume, seems to greatly underestimate the fluctuation intensity in dispersion in pipe flow.

Generally, increasing the Reynolds numbers for free turbulent mixing zones results in more rapid decay of maximum fluctuation intensity. Variations in Reynolds number have appreciable effect on the intensity profiles only for moderately turbulent flows in which the Reynolds number is less than about 1 to 2×10^4.

Practical difficulties involved in determining the initial

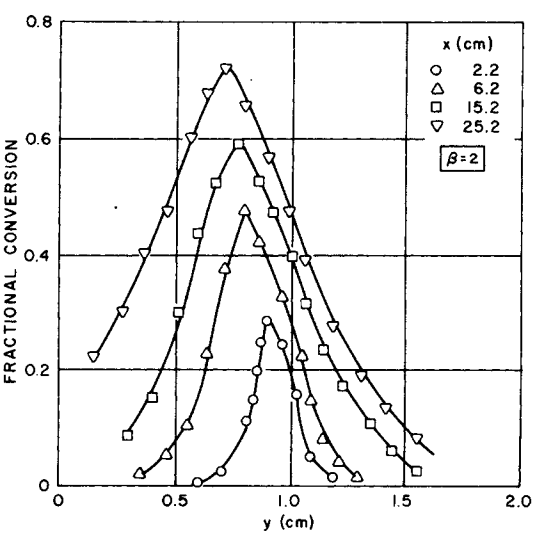

Fig. 22. Fractional conversion profiles for the mixing zone conditions of Figure 21 with $\beta = 2$.

fluctuation variance limit the quantitative applicability of Toor's model relating accomplished mixing and fractional conversion to rather ideal flows. However, better developed free turbulence characteristics leading to more rapid fluctuation decay in mixing lead to increased conversion in the equivalent reacting system. For reaction in the mixing zone, changing the ratio of initial reactant concentrations from 1 to 2 is more effective in increasing fractional conversion at higher Reynolds numbers, that is, in more fully developed free mixing zones.

ACKNOWLEDGMENT

Acknowledgment is made to the donors of the Petroleum Research Fund, administered by the American Chemical Society, for support of this research.

NOTATION

C = concentration
d = diameter
D = diffusivity
e = voltage fluctuation
E = voltage
F = fractional conversion
I_s = intensity of segregation
L_γ = concentration of macroscale
M = mesh size
N_{Re} = Reynolds number
N_{Sc} = Schmidt number
R_D = detector resistance
R_p = resistance measured with conductivity probe
t = time
u_i = i^{th} component of fluctuating velocity
$\overline{U}$ = mean velocity
x_i = component of spatial coordinates
x = axial position from origin along mean flow direction, downstream
y = lateral position

Greek Letters

β = stoichiometric parameter
γ = concentration fluctuation
$\sqrt{\overline{\gamma^2}}$ = root-mean-square concentration fluctuation, or intensity
ϵ = viscous dissipation rate
$\lambda_\gamma, \lambda_g$ = microscales for concentration and velocity
ν = kinematic viscosity
τ = decay time constant, homogenization

Subscripts

D = duct or pipe
i = vector component or initial value
j = jet
m = maximum or center-line value
o = origin
s = secondary flow

LITERATURE CITED

1. Rosensweig, R. E., H. C. Hottel, and G. C. Williams, *Chem. Eng. Sci.*, **15**, 111 (1961).
2. Wilson, R. A. M., and P. V. Danckwerts, *ibid.*, **19**, 885 (1964).
3. Becker, H. A., H. C. Hottel, and G. C. Williams, "Eleventh Symposium (International) on Combustion," p. 791, the Combustion Institute (1967).
4. ———, *J. Fluid Mech.*, **30**, 259 (1967).
5. Lee, Jon, and R. S. Brodkey, *AIChE J.*, **10**, 187 (1964).
6. Becker, H. A., R. E. Rosensweig, and J. R. Gwozdz, *ibid.*, **12**, 965 (1966).
7. Gibson, C. H., and W. H. Schwarz, *J. Fluid Mech.*, **16**, 357, 365 (1963).
8. Keeler, R. N., E. E. Petersen, and J. M. Prausnitz, *AIChE J.*, **11**, 221 (1965).
9. Townsend, A. A., "The Structure of Turbulent Shear Flow," Cambridge University Press, England (1953).
10. Hinze, J. O., "Turbulence," McGraw-Hill, New York (1959).
11. Corrsin, Stanley, "Handbuch der Physik," Vol. 8/2, p. 524, Springer-Verlag, Germany (1963).
12. Rosler, R. S., and S. G. Bankoff, *AIChE J.*, **9**, 672 (1963).
13. Sami, S., T. Carmody, and H. Rouse, *J. Fluid Mech.*, **27**, 231 (1967).
14. Heskestad, G., *J. Appl. Mech.*, **32**, 721 (1965).
15. Csanady, G. R., *J. Fluid Mech.*, **15**, 545 (1963).
16. Corrsin, Stanley, *J. Aeronaut. Sci.*, **18**, 417 (1951).
17. ———, *AIChE J.*, **3**, 329 (1957).
18. *Ibid.*, **10**, 870 (1964).
19. Mills, R. R., Jr., A. L. Kistler, V. O'Brien, and Stanley Corrsin, *Natl. Advisory Comm. Aeronaut. Tech. Note 4288* (Aug., 1958).
20. Batchelor, G. K., *J. Fluid Mech.*, **5**, 113 (1959).
21. ———, I. D. Howells, and A. A. Townsend, *ibid.*, 134.
22. Pao, Y. H., *Phys. Fluids*, **8**, 1063 (1965).
23. Lee, Jon, *ibid.*, 1647.
24. Lanza, J., and W. H. Schwarz, "The Scalar Spectrum for the Equilibrium Range of Wave Numbers," Stanford Univ., Calif., (Sept., 1966).
25. Beek, John, Jr., and R. S. Miller, *Chem. Eng. Progr. Symposium Ser. No. 25*, **55**, 23 (1959).
26. Brodkey, R. S., in "Mixing—Theory and Practice," Vol. I, V.W. Uhl and J. B. Gray, eds., Academic Press, New York (1966).
27. Howells, I. D., *J. Fluid Mech.*, **9**, 104 (1960).
28. Danckwerts, P. V., *Appl. Sci. Res.*, **A3**, 279 (1953).
29. Brodkey, R. S., *AIChE J.*, **12**, 403 (1966).
30. ———, and J. P. Gegner, *ibid.*, 817.
31. Nye, J. O., and R. S. Brodkey, *J. Fluid Mech.*, **29**, 151 (1967).
32. Frenkiel, F. N., in "Advances in Applied Mechanics," Vol. 3, Academic Press, New York (1953).
33. Csanady, G. T., *J. Atmos. Sci.*, **24**, 21 (1967).
34. Vassilatos, George, and H. L. Toor, *AIChE J.*, **11**, 666, (1965).
35. Torrest, R. S., Ph.D. thesis, Univ. Minn., Minneapolis (1967).
36. Toor, H. L., *AIChE J.*, **8**, 70 (1962).
37. Becker, H. A., H. C. Hottel, and G. C. Williams, *J. Fluid Mech.*, **30**, 259 (1967).
38. ————————, "Ninth International Symposium on Combustion," p. 7, Academic Press, New York (1963).
39. ————————, "Tenth Symposium (International) on Combustion," p. 1253, the Combustion Institute, Pittsburgh (1965).
40. Lawrence, W. J., Ph.D. thesis, Univ. Calif., Berkeley (1965).
41. Forstall, W., Jr., and A. H. Shapiro, *J. Appl. Mech.*, **17**, 399 (1950).
42. Hinze, J. O., and B. G. van der Hegge Zijnen, *Appl. Sci. Res.*, **A1**, 435 (1949).
43. Flint, D. L., Hisao Kada, and T. J. Hanratty, *AIChE J.*, **6**, 325 (1960).
44. Van der Hegge Zijnen, B. G., *Appl. Sci. Res.*, **A7**, 256 (1957).
45. Kristmanson, D., and P. V. Danckwerts, *Chem. Eng. Sci.*, **16**, 267 (1961).
46. Saidel, G. M., and H. E. Hoelscher, *AIChE J.*, **11**, 1058 (1965).
47. Crum, G. F., and T. J. Hanratty, *Appl. Sci. Res.*, **A15**, 177 (1965).
48. Torrest, R. S., and W. E. Ranz, *Ind. Eng. Chem. Fundamentals*, **8**, 810 (1969).

Manuscript received June 4, 1968; revision received February 18, 1969; paper accepted February 20, 1969.